

# Scaling Laws of Polyelectrolyte Adsorption

Itamar Borukhov and David Andelman\*

*School of Physics and Astronomy, Raymond and Beverly Sackler Faculty of Exact Sciences, Tel-Aviv University, Ramat-Aviv 69978, Tel-Aviv, Israel*

Henri Orland

*Service de Physique Théorique, CEA, CE-Saclay, 91191 Gif-sur-Yvette Cedex, France*

(June 9, 2022)

Adsorption of charged polymers (polyelectrolytes) from a semi-dilute solution to a charged surface is investigated theoretically. We obtain simple scaling laws for (i) the amount of polymer  $\Gamma$  adsorbed to the surface and (ii) the width  $D$  of the adsorbed layer, as function of the fractional charge per monomer  $p$  and the salt concentration  $c_b$ . For strongly charged polyelectrolytes ( $p \lesssim 1$ ) in a low-salt solution, both  $\Gamma$  and  $D$  scale as  $p^{-1/2}$ . In salt-rich solutions  $D \sim c_b^{1/2}/p$  whereas the scaling behavior of  $\Gamma$  depends on the strength of the polymer charge. For weak polyelectrolytes ( $p \ll 1$ ) we find that  $\Gamma \sim p/c_b^{1/2}$  while for strong polyelectrolytes  $\Gamma \sim c_b^{1/2}/p$ . Our results are in good agreement with adsorption experiments and with numerical solutions of mean-field equations.

## I. INTRODUCTION

Polyelectrolytes (charged polymers) are widely used in industrial applications. For example, many colloidal suspensions can be stabilized by the adsorption of polyelectrolytes. In many experiments, the total amount of polymer adsorbed on a surface (the polymer *surface excess*) is measured as a function of the bulk polymer concentration, pH and/or ionic strength of the bulk solution [1–8]. (For reviews see, e.g., refs. [9–12]). More recently, spectroscopy [3] and ellipsometry [7] have been used to measure the width of the adsorbed polyelectrolyte layer. Other techniques such as neutron scattering can be employed to measure the entire profile of the adsorbed layer [13,14].

The theoretical treatment of polyelectrolytes in solution is not very well established because of the delicate interplay between the chain connectivity and the long range nature of electrostatic interactions [15–18]. In many studies adsorption of polyelectrolytes is treated as an extension of neutral polymer theories. In these approaches the polymer concentration profile is determined by minimizing the overall free energy.

One approach is a discrete *multi-Stern layer* model [19–23], where the system is placed on a lattice whose sites can be occupied by a monomer, a solvent molecule or a small ion. The electrostatic potential is determined self-consistently together with the concentration profiles of the polymer and the small ions. Another approach treats the electrostatic potential and the polyelectrolyte concentration as continuous functions [24–28]. These quantities are obtained from two coupled differential equations derived from the total free energy of the system.

In the present work we focus on the adsorption behavior of polyelectrolytes near a single charged surface held at a constant potential. Simple scaling expressions are presented and compared to concentration profiles that we obtain from exact numerical solutions, and to experiments measuring the amount of polymer adsorbed on the surface. In Sec. I the adsorption problem is treated numerically. We then present in Sec. II simple scaling arguments describing the adsorption characteristics and in Sec. III we compare our scaling results to experiments. Finally, we present our conclusions and some future prospects.

## II. NUMERICAL PROFILES

Consider a semi-dilute solution of polyelectrolytes in good solvent in contact with a charged surface (Fig. 1). In addition to the polymer chains and their counterions, the solution contains small ions (salt) assumed hereafter to be monovalent. The system is coupled to a bulk reservoir containing polyelectrolyte chains and salt. In the present work we assume that the charge density on the polymer chains is continuous and uniformly distributed along the chains. This assumption is valid as long as the electrostatic potential is not too high,  $|\beta e\psi| < 1$ , where  $1/\beta = k_B T$  is the thermal energy,  $e$  is the electron charge and  $\psi$  is the electrostatic potential. Further treatments of the polymer charge distribution (annealed and quenched models) can be found in refs. [27,28].

Within mean-field approximation, the free energy of the system can be expressed in terms of the local electrostatic potential  $\psi(\mathbf{r})$ , the local monomer concentration  $\rho_m(\mathbf{r})$  and the local concentration of positive and negative ions  $c^\pm(\mathbf{r})$ .

It is convenient to introduce the polymer order parameter  $\phi(\mathbf{r})$  where  $\rho_m(\mathbf{r}) = |\phi(\mathbf{r})|^2$ . The excess free energy with respect to the bulk  $F$  is then [25–28]

$$F = \int d\mathbf{r} \{f_{pol}(\mathbf{r}) + f_{ions}(\mathbf{r}) + f_{el}(\mathbf{r})\} \quad (1)$$

The polymer contribution is

$$f_{pol}(\mathbf{r}) = k_B T \left[ \frac{a^2}{6} |\nabla\phi|^2 + \frac{1}{2} v(\phi^4 - \phi_b^4) \right] - \mu_p(\phi^2 - \phi_b^2) \quad (2)$$

where the first term is the polymer elastic energy,  $a$  being the effective monomer size. The second term is the excluded volume contribution where  $v \sim a^3$ . The last term couples the system to the reservoir, where  $\mu_p$  is the chemical potential of the polymers and  $\rho_m(\infty) = \phi_b^2$  is the bulk monomer concentration.

The entropic contribution of the small (monovalent) ions is

$$f_{ions}(\mathbf{r}) = \sum_{i=\pm} k_B T [c^i \ln c^i - c^i - c_b^i \ln c_b^i + c_b^i] - \mu^i(c^i - c_b^i) \quad (3)$$

where  $c^i(\mathbf{r})$ ,  $c_b^i$  and  $\mu^i$  are, respectively, the local concentration, the bulk concentration and the chemical potential of the  $i = \pm$  ions.

Finally, the electrostatic contributions is

$$f_{el}(\mathbf{r}) = p e \phi^2 \psi + e c^+ \psi - e c^- \psi - \frac{\varepsilon}{8\pi} |\nabla\psi|^2 \quad (4)$$

The first three terms are the electrostatic energies of the monomers, the positive ions and the negative ions, respectively,  $p$  is the fractional charge carried by one monomer. The last term is the self energy of the electric field where  $\varepsilon$  is the dielectric constant of the solution. Note that the electrostatic contribution, eq. 4, is equivalent to the well known result:  $F_{el} = (\varepsilon/8\pi) \int d\mathbf{r} |\nabla\psi|^2$  plus surface terms. This can be seen by substituting the Poisson–Boltzmann equation (as obtained below) into eq. 4 and then integrating by parts.

Minimization of the free energy with respect to  $c^\pm$ ,  $\phi$  and  $\psi$  yields a Boltzmann distribution for the density of the small ions,  $c^\pm(\mathbf{r}) = c_b^\pm \exp(\mp\beta e\psi)$ , and two coupled differential equations for  $\phi$  and  $\psi$ :

$$\nabla^2 \psi(\mathbf{r}) = \frac{8\pi e}{\varepsilon} c_b \sinh(\beta e\psi) - \frac{4\pi e}{\varepsilon} (p\phi^2 - p\phi_b^2 e^{\beta e\psi}) \quad (5)$$

$$\frac{a^2}{6} \nabla^2 \phi(\mathbf{r}) = v(\phi^3 - \phi_b^2 \phi) + p\phi\beta e\psi \quad (6)$$

Equation 5 is a generalized Poisson–Boltzmann equation including the free ions as well as the charged polymers. The first term represents the salt contribution and the second term is due to the charged monomers and their counter-ions. Equation 6 is a generalization of the self-consistent field equation of neutral polymers [16]. In the bulk, the above equations are satisfied by setting  $\psi \rightarrow 0$  and  $\phi \rightarrow \phi_b$ .

When a polyelectrolyte solution is in contact with a charged surface, the chains will adsorb to (or deplete from) the surface, depending on the nature of the monomer–surface interactions. The large number of monomers on each polymer chain enhances these interactions. For simplicity, we assume that the surface is ideal, *i.e.*, flat and homogeneous. In this case physical quantities depend only on the distance  $x$  from the surface (see Fig. 1). The surface imposes boundary conditions on the polymer order parameter  $\phi(x)$  and electrostatic potential  $\psi(x)$ . In thermodynamic equilibrium all charge carriers in solution should exactly balance the surface charges (charge neutrality). The self-consistent field equation, the Poisson–Boltzmann equation and the boundary conditions uniquely determine the polymer concentration profile and the electrostatic potential. In most cases, these two coupled non-linear equations can only be solved numerically.

In the present work we have chosen the surface to be at a constant potential  $\psi_s$ , leading to the following electrostatic boundary condition [29]

$$\psi|_{x=0} = \psi_s \quad (7)$$

The boundary conditions for  $\phi(x)$  depend on the nature of the short range interaction of the monomers and the surface. For simplicity, we take a non-adsorbing surface and require that the monomer concentration will vanish there:

$$\phi|_{x=0} = 0 \quad (8)$$

Far from the surface ( $x \rightarrow \infty$ ) both  $\psi$  and  $\phi$  reach their bulk values and their derivatives vanish:  $\psi'|_{x \rightarrow \infty} = 0$  and  $\phi'|_{x \rightarrow \infty} = 0$ .

Figure 2 shows several adsorption profiles obtained from numerical solutions of the mean-field equations (eqs. 5, 6) using a minimal squares method. The polymer is positively charged and is attracted to the non-adsorbing surface held at a constant negative potential. The aqueous solution contains a small amount of monovalent salt ( $c_b = 0.1\text{mM}$ ). The reduced concentration profile  $c(x)/\phi_b^2$  is plotted as a function of the distance from the surface. Different curves correspond to different values of the reduced surface potential  $y_s = \beta e\psi_s$ , the charge fraction  $p$  and the monomer size  $a$ . Although the spatial variation of the profiles differs in detail, they all have a single peak characterized by an adsorption length. We use this feature in the next section to obtain simple analytical expressions characterizing the adsorption.

### III. SCALING RESULTS

The difficulty in obtaining a simple picture of polyelectrolyte adsorption lies in the existence of several length scales in the problem: (i) the Edwards correlation length  $\xi = a/(v\phi_b^2)^{1/2}$ , characterizing the concentration fluctuations of neutral polymer solutions; (ii) the Debye-Hückel screening length  $\kappa_s^{-1} = (8\pi l_B c_b)^{-1/2}$  where  $l_B = e^2/\epsilon k_B T$  is the Bjerrum length equal to about  $7\text{\AA}$  for aqueous solutions at room temperature. Additional length scales can be associated with electrostatic and/or short range surface interactions.

Motivated by the numerical results (Fig. 2), we assume that the balance between these interactions results in one dominant length scale  $D$  characterizing the adsorption at the surface. Hence, we write the polymer order parameter profile in the form of

$$\phi(x) = \sqrt{c_m} h(x/D) \quad (9)$$

where  $h(z)$  is a dimensionless function normalized to one at its maximum and  $c_m$  sets the scale of polymer adsorption. The free energy can be now expressed in terms of  $D$  and  $c_m$  while the exact form of  $h(z)$  affects only the numerical prefactors.

In principle, the adsorption length  $D$  depends also on the ionic strength through  $\kappa_s^{-1}$ . As discussed below the scaling assumption (eq. 9) is only valid as long as  $\kappa_s^{-1}$  and  $D$  are not of the same order of magnitude. Otherwise,  $h$  should depend on both  $\kappa_s x$  and  $x/D$ . We concentrate now on two limiting regimes where eq. 9 can be justified: (i) the low-salt regime  $D \ll \kappa_s^{-1}$  and (ii) the salt-rich regime  $D \gg \kappa_s^{-1}$ .

#### A. Low-Salt Regime; $D \ll \kappa_s^{-1}$

In the low-salt regime the effect of the small ions can be neglected and the free energy, eqs. 1-4, is approximated by (see also ref. [26])

$$\beta F = A_1 \frac{a^2}{6D} c_m - A_2 p |y_s| c_m D + 4\pi B_1 l_B p^2 c_m^2 D^3 + \frac{1}{2} B_2 v c_m^2 D \quad (10)$$

The first term is the elastic energy characterizing the response of the polymer to concentration inhomogeneities. The second term accounts for the electrostatic attraction of the polymers to the charged surface. The third term represents the Coulomb repulsion between adsorbed monomers. Indeed, the interaction between two layers with surface charge densities  $\sigma = pe\phi^2(x)dx$  and  $\sigma' = pe\phi^2(x')dx'$  is proportional to the distance  $|x - x'|$  yielding the  $D^3$  dependence. The last term represents the excluded volume repulsion between adsorbed monomers, where we assume that the monomer concentration near the surface is much larger than the bulk concentration  $c_m \gg \phi_b^2$ . The coefficients  $A_1, A_2, B_1$  and  $B_2$  are numerical prefactors, which depend on the exact shape of the dimensionless function  $h(z)$ . These coefficients can be explicitly calculated for a specific profile by integrating the Poisson equation without taking into account the small ion contributions [31]. For a linear profile,  $h(z) = z$  for  $0 \leq z \leq 1$  and  $h(z) = 0$  for  $z > 1$ , we get  $A_1 = 1, A_2 = 1/3, B_1 = 1/14$  and  $B_2 = 1/5$ ; For a parabolic profile,  $h(z) = 4z(1 - z)$  for  $0 \leq z \leq 1$  and  $h(z) = 0$  for  $z > 1$ , we get  $A_1 = 16/3, A_2 = 8/15, B_1 \simeq 1/9$  and  $B_2 \simeq 2/5$ .

In the low-salt regime and for strong enough polyelectrolytes the electrostatic interactions are much stronger than the excluded volume ones. Neglecting the latter interactions and minimizing the free energy with respect to  $D$  and  $c_m$  gives:

$$D^2 = \frac{5A_1}{6A_2} \frac{a^2}{p|y_s|} \sim \frac{1}{p|y_s|} \quad (11)$$

and

$$c_m = \frac{12A_2^2}{25A_1B_1} \frac{|y_s|^2}{4\pi l_B a^2} \sim |y_s|^2 \quad (12)$$

The above expressions are valid as long as (i)  $D \ll \kappa_s^{-1}$  and (ii) the excluded volume term in eq. 10 is negligible. The former condition translates into  $c_b \ll p|y_s|/(8\pi l_B a^2)$ . For  $|y_s| \simeq 1$ ,  $a = 5\text{\AA}$  and  $l_B = 7\text{\AA}$  this limits the salt concentration to  $c_b/p \ll 0.4$  M. The latter condition on the magnitude of the excluded volume term can be shown to be equivalent to  $p \gg v|y_s|/l_B a^2$ . These requirements are consistent with the data presented in Fig. 2.

We recall that the profiles presented in Fig. 2 were obtained from the numerical solution of eqs. 5 and 6, including the effect of small ions and excluded volume. The scaling relations are verified by plotting in Fig. 3 the same sets of data as in Fig. 2 using rescaled variables as defined in eqs. 11,12. Namely, the rescaled electrostatic potential  $\psi(x)/\psi_s$  and polymer concentration  $c(x)/c_m \sim c(x)a^2/|y_s|^2$  are plotted as functions of the rescaled distance  $x/D \sim xp^{1/2}|y_s|^{1/2}/a$ . The different curves roughly collapse on the same curve.

In many experiments the total amount of adsorbed polymer per unit area  $\Gamma$  is measured. Our scaling assumption yields

$$\Gamma = \int_0^\infty [c(x) - \phi_b^2] dx \simeq Dc_m \simeq \frac{|y_s|^{3/2}}{l_B a p^{1/2}} \sim \frac{|y_s|^{3/2}}{p^{1/2}} \quad (13)$$

The adsorbed amount  $\Gamma(p)$  in the low-salt regime is plotted in the inset of Fig. 4a. One of the important features is the decrease in  $\Gamma$  with increasing charge fraction  $p$ . This can be understood in the following way: the monomer-monomer Coulomb repulsion scales as  $(pc_m)^2$ , and dominates over the adsorption energy scaling only as  $pc_m$ .

### B. Salt-Rich Regime; $D \gg \kappa_s^{-1}$

The opposite case occurs when  $D$  is much larger than  $\kappa_s^{-1}$ . In this case the electrostatic interactions are short ranged with a cut-off  $\kappa_s^{-1}$  [26]. The free energy then reads:

$$\beta F = A_1 \frac{a^2}{6D} c_m - A_2 p |y_s| c_m \kappa_s^{-1} + 4\pi B_1 l_B p^2 \kappa_s^{-2} c_m^2 D + \frac{1}{2} B_2 v c_m^2 D \quad (14)$$

Note that  $\kappa_s^{-1}$  enters in the 2nd and 3rd terms. The third term can be viewed as an additional electrostatic excluded volume with  $v_{el} \sim l_B (p/\kappa_s)^2$ .

Minimization of the free energy gives

$$D = \frac{A_1}{2A_2} \frac{\kappa_s a^2}{p|y_s|} \sim \frac{c_b^{1/2}}{p|y_s|} \quad (15)$$

and

$$c_m \sim \frac{p^2 |y_s|^2 / (\kappa_s a)^2}{B_1 p^2 / c_b + B_2 v} \quad (16)$$

yielding

$$\Gamma \sim \frac{p|y_s|c_b^{-1/2}}{B_1 p^2 / c_b + B_2 v} \quad (17)$$

The adsorption behavior is depicted in Figs. 4 and 5. Our results are in agreement with numerical solutions of discrete lattice models (the multi-Stern layer theory) [9–11,19–23]. In Fig. 4  $\Gamma$  is plotted as function of  $p$  (Fig. 4a) and pH (Fig. 4b) for three different salt concentrations. The behavior as seen on Fig. 4b represents annealed polyelectrolytes where the nominal charge fraction is controlled by the pH of the solution through

$$p = \frac{10^{\text{pH}-\text{pK}_0}}{1 + 10^{\text{pH}-\text{pK}_0}} \quad (18)$$

where  $pK_0 = -\log_{10} K_0$  and  $K_0$  is the apparent dissociation constant.

Another interesting observation which can be deduced from eq. 17 is that  $\Gamma$  is only a function of  $p/\sqrt{c_b}$ . Indeed, as can be seen in Fig. 4,  $c_b$  only affects the position of the peak and not its height.

The effect of salt concentration is shown in Fig. 5, where  $\Gamma$  is plotted in 5a as function of the salt concentration  $c_b$  for two charge fractions  $p = 0.01$  and  $0.25$ . In Fig. 5b,  $D$  is plotted for the same range of  $c_b$  and for  $p = 0.1$ . The solid curves are obtained within the salt-rich regime (eq. 17).

The extrapolation of the salt-rich expression eq. 17 towards low values of  $c_b$  does not give the correct low-salt limit, because the basic assumptions of the salt-rich regime are no longer valid. Instead, a simple interpolation [32] between the low-salt and salt-rich regimes is used in the same figure (dashed curves). It demonstrates a plausible behavior of  $\Gamma$  and  $D$  for intermediate salt concentrations where our above scaling expressions are not valid. At low salt concentrations,  $\Gamma$  is almost independent of  $c_b$  and saturates to the low-salt value (left hand side of Fig. 5a). At high salt concentrations, the salt-rich result is recovered (right hand side of Fig. 5a). For weak polyelectrolytes (e.g.,  $p = 0.01$  in Fig. 5a), addition of salt weakens the surface attraction. Consequently,  $\Gamma$  is a decreasing function of  $c_b$  in the whole  $c_b$  range. For strong polyelectrolytes, (e.g.,  $p = 0.25$  in Fig. 5a),  $\Gamma$  is an increasing function of  $c_b$  at low salt concentrations and a decreasing function at high salt concentrations. As a result, there is a maximum in  $\Gamma$  at some intermediate value of  $c_b$ .

From Figs. 4, 5a and eq. 17, it is clear that the salt-rich regime can be divided into two sub regimes according to the polyelectrolyte charge. At low charge fractions (sub-regime SR I),  $p \ll p^* = (c_b v)^{1/2}$ , the excluded volume term dominates the denominator of eq. 17 and

$$\Gamma \sim \frac{p|y_s|}{c_b^{1/2}} \quad (19)$$

whereas at high  $p$  (sub-regime SR II),  $p \gg p^*$ , the monomer-monomer electrostatic repulsion dominates and  $\Gamma$  decreases with  $p$  and increases with  $c_b$ :

$$\Gamma \sim \frac{c_b^{1/2}|y_s|}{p} \quad (20)$$

The various regimes with their crossover lines are shown schematically in Fig. 6.

#### IV. COMPARISON TO EXPERIMENT

The scaling behavior found in the previous section can be divided into three distinct regimes (Fig. 6):

1. Low-Salt regime  $c_b \ll p|y_s|/8\pi l_B a^2$ .
2. First salt-rich (SR I) regime, where  $c_b \gg p|y_s|/8\pi l_B a^2$  and  $p \ll p^* = (c_b v)^{1/2}$  (weak polyelectrolytes).
3. Second salt-rich (SR II) regime, where  $c_b \gg p|y_s|/8\pi l_B a^2$  and  $p \gg p^*$  (strong polyelectrolytes).

Our scaling results are in good agreement with adsorption experiments, although in experiments the charge distribution of the polyelectrolytes can be more complicated.

##### A. Low-Salt Regime

Denoyel et al. [4] have studied the adsorption of heteropolymers made of neutral (acrylamide) and cationic monomers (derived from chloride acrylate). The fractional charge was fixed during the polymerization process and varied from  $p = 0$  to 1. Since the salt amount in their experiment was quite low: 1.2mM corresponding to  $\kappa_s^{-1} \simeq 90\text{\AA}$ , their experimental range satisfies the low-salt conditions. Indeed, the measured  $\Gamma$  (Table II in ref. [4]) exhibits a  $p^{-1/2}$  dependence as in eq. 13.

## B. Weak Polyelectrolytes: Effect of Salt

Shubin and Linse [7] adsorbed another cationic derivative of poly(acrylamide) on silica. The fractional charge was fixed at a low value ( $p = 0.034$ ), while the salt concentration varied from  $c_b = 0.1\text{mM}$  to  $c_b \approx 0.2\text{M}$ . Ellipsometry was used to measure  $\Gamma$  and  $D$  of the adsorbed layer as function of the salt concentration. This low charge fraction belongs to the left side (low  $p$ ) of Fig. 6. The experimental behavior is similar to our predictions as shown in Fig. 5 for weak polyelectrolytes. At low electrolyte concentration ( $c_b < 1\text{mM}$ ), the adsorbed amount is essentially constant and decreases at higher salt concentration (SR I regime of Fig. 6). Similar behavior was obtained both by numerical calculations using the multi-Stern layer model [7,22,23], and in other adsorption experiments of cationic potato starch [6].

## C. Strong Polyelectrolytes: Effect of Salt

Kawaguchi et al. [2] measured the adsorption of a highly charged polyelectrolyte (PVPP) on silica surfaces. Due to the high ionic strength this system belongs to the SR II regime. Indeed,  $\Gamma \sim \sqrt{c_b}$  was found in agreement with our prediction. Meadows et al. [3] also performed adsorption experiments with highly charged ( $p = 0.9$ ) hydrolyzed poly(acrylamide). The adsorbed amount  $\Gamma$  and the width of the adsorbed layer  $D$  were found to increase upon addition of salt. Qualitatively, this agrees with our prediction in the SR II regime. However, the measured power laws are weaker than our predictions. A simple power law fit of their salt dependence gives  $\Gamma \sim c_b^{1/4}$  as compared to our  $c_b^{1/2}$  prediction. This behavior is intermediate between the salt free and SR II regimes.

## D. Effect of Charge Fraction

Peysers and Ullman [1] studied the adsorption of PVP on a glass surface as function of the charge fraction for three different salt concentrations. The system belongs to the right side ( $p \lesssim 1$ ) of Fig. 5 between the low-salt and SR II regimes. As expected  $\Gamma$  increases with  $c_b$  and decreases with  $p$ . Moreover, it is possible to fit the data to a simple scaling law of the form  $\Gamma \sim c_b^{1/4}/p^{1/2}$ . Our scaling results do not fit very well these experiments which lie in the intermediate regime, between the low-salt and SR II regimes.

In experiments on annealed polyelectrolytes [5,8], the polymer charge can be tuned by the pH of the solution (eq. 18). The behavior then shifts continuously from the SR I to the SR II regimes. For example, Blaakmeer et al. [5] used polyacrylic acid which is neutral (no dissociation) at low pH but becomes negatively charged (strong dissociation) at higher pH. As predicted by eq. 17 (see also Fig. 4b), a non-monotonous dependence of  $\Gamma$  on the pH was observed, with a maximum below the  $\text{pK}_0$ . This effect had been already verified by numerical calculations based on the multi-Stern layer model [5].

A similar maximum in  $\Gamma$  was also observed in adsorption experiments of proteins [12] and diblock copolymers with varying ratios between the charged and neutral blocks [8] and may be interpreted using similar considerations.

## V. CONCLUSIONS

In this work we use simple arguments to derive scaling laws describing the adsorption of polyelectrolytes on a single charged surface held at a constant potential. We obtain expressions for the amount of adsorbed polymer  $\Gamma$  and the width  $D$  of the adsorbed layer, as a function of the fractional charge  $p$  and the salt concentration  $c_b$ . In the low-salt regime a  $p^{-1/2}$  dependence of  $\Gamma$  is found. It is supported by our numerical solutions of the profile equations 5, 6 and is in agreement with experiment [4]. This behavior is due to strong Coulomb repulsion between adsorbed monomers in the absence of salt. As  $p$  decreases, the adsorbed amount increases until the electrostatic attraction becomes weaker than the excluded volume repulsion, at which point,  $\Gamma$  starts to decrease rapidly. At high salt concentrations we obtain two limiting behaviors: (i) for weak polyelectrolytes,  $p \ll p^* = (c_b v)^{1/2}$ , the adsorbed amount increases with the fractional charge and decreases with the salt concentration,  $\Gamma \sim p/\sqrt{c_b}$ , due to the monomer-surface electrostatic attraction. (ii) For strong polyelectrolytes,  $p \gg p^*$ , the adsorbed amount decreases with the fractional charge and increases with the salt concentration,  $\Gamma \sim \sqrt{c_b}/p$ , due to the dominance of the monomer-monomer electrostatic repulsion. Between these two regimes we find that the adsorbed amount reaches a maximum in agreement with experiments [5,8].

The scaling approach can serve as a starting point for further investigations. Special attention should be directed to the crossover regime where  $D$  and  $\kappa_s^{-1}$  are of comparable size. At present, it is not clear whether the intermediate regime represents simply a crossover between regimes or is a scaling regime on its own. Another important question addresses the relative importance of attractive versus repulsive forces between two charged surfaces in presence of a polyelectrolyte solution. Finally, our approach could be used in non flat geometries such as spheres (colloidal particles) and cylinders.

#### Acknowledgments

We would like to thank L. Auvray, M. Cohen-Stuart, J. Daillant, H. Diamant, P. Guenoun, Y. Kantor, P. Linse, P. Pincus, S. Safran and C. Williams for useful discussions. Two of us (IB and DA) would like to thank the Service de Physique Théorique (CE-Saclay) and one of us (HO) the Sackler Institute of Solid State Physics (Tel Aviv University) for their hospitality. Partial support from the German-Israel Foundation (G.I.F) under grant No. I-0197 and the U.S.-Israel Binational Foundation (B.S.F.) under grant No. 94-00291 is gratefully acknowledged.

- [1] Peyser P. and Ullman R., *J. Pol. Sci. A* **1965**, *3*, 3165.
- [2] Kawaguchi M., Kawaguchi H. and Takahashi A., *J. Coll. Interface Sci.* **1988**, *124*, 57.
- [3] Meadows J., Williams P. A., Garvey M. J., Harrop R. and Phillips G. O., *J. Coll. Interface Sci.* **1989**, *132*, 319.
- [4] Denoyel R., Durand G., Lafuma F. and Audbert R., *J. Coll. Interface Sci.* **1990**, *139*, 281.
- [5] Blaakmeer J., Böhmer M. R., Cohen Stuart M. A. and Fleer G. J., *Macromolecules* **1990**, *23*, 2301.
- [6] Van de Steeg H. G. M., de Keizer A., Cohen Stuart M. A., and Bijsterbosch B. H., *Coll. Surf. A* **1993**, *70*, 91.
- [7] Shubin V. and Linse P., *J. Phys. Chem.* **1995**, *99*, 1285.
- [8] Hoogeveen N. G., Ph.D. Thesis, Wageningen Agricultural University, The Netherlands, 1996.
- [9] Cohen Stuart M. A., *J. Phys. France* **1988**, *49*, 1001.
- [10] Cohen Stuart M. A., Fleer G. J., Lyklema J., Norde W. and Scheutjens J. M. H. M., *Adv. Coll. Interface Sci.* **1991**, *34*, 477.
- [11] Fleer G. J., Cohen Stuart M. A., Scheutjens J. M. H. M., Cosgrove T. and Vincent B., *Polymers at Interfaces*; Chapman & Hall: London, 1993; chapter 11.
- [12] Haynes C. A. and Norde W., *Coll. Surf. B* **1994**, *2*, 517.
- [13] Auroy P., Auvray L. and Léger L., *Macromolecules* **1991**, *24*, 2523.
- [14] Guiselin O., Lee L. T., Farnoux B. and Lapp A., *J. Chem. Phys.* **1991**, *95*, 4632.
- [15] Oosawa F., *Polyelectrolytes*; Marcel Dekker: New York, 1971.
- [16] De Gennes P. G., *Scaling Concepts in Polymer Physics*; Cornell Univ.: Ithaca, 1979.
- [17] Odijk T., *Macromolecules* **1979**, *12*, 688.
- [18] Dobrynin A. V., Colby R. H. and Rubinstein M., *Macromolecules* **1995**, *28*, 1859.
- [19] Van der Schee H. A. and Lyklema J., *J. Phys. Chem.* **1984**, *88*, 6661.
- [20] Papenhuijzen J., Van der Schee H. A. and Fleer G. J., *J. Coll. Interface Sci.* **1985**, *104*, 540.
- [21] Evers O. A., Fleer G. J. Scheutjens J. M. H. M. and Lyklema J., *J. Coll. Interface Sci.* **1985**, *111*, 446.
- [22] Van de Steeg H. G. M., Cohen Stuart M. A., de Keizer A. and Bijsterbosch B. H., *Langmuir* **1992**, *8*, 8.
- [23] Linse P., *Macromolecules* **1996**, *29*, 326.
- [24] Muthukumar M., *J. Chem. Phys.* **1987**, *86*, 7230.
- [25] Varoqui R., Johner A. and Elaissari A., *J. Chem. Phys.* **1991**, *94*, 6873.
- [26] Varoqui R., *J. Phys. (France) II* **1993**, *3*, 1097.
- [27] Borukhov I., Andelman D. and Orland H., *Europhys. Lett.* **1995**, *32*, 499; Borukhov I., Andelman D. and Orland H., in *Short and Long Chains at Interfaces*, eds. Daillant J., Guenoun P., Marques C., Muller P. and Trần Thanh Vân J. (Edition Frontieres, Gif-sur-Yvette, 1995) pp. 13-20.
- [28] Borukhov I., Andelman D. and Orland H., *unpublished*.
- [29] It is also possible to use a constant surface charge density  $\sigma$ . The boundary condition then becomes  $\psi'|_s = -4\pi\sigma/\epsilon$ . In real systems, some of the ionized surface sites can be neutralized by the binding of small ions from the solution. The actual surface charge is not fixed but depends on the surface potential [30]. Neither the surface potential nor the surface charge are fixed, and the boundary conditions are mixed. The choice of simple boundary conditions is only an approximation of a real surface-solution system. The quality of the approximation depends on the details of the experimental system.
- [30] For a review see: Israelachvili J. N., *Intermolecular and Surface Forces*, 2nd ed.; Academic Press: London, 1990.
- [31] For a given profile  $h(x/D)$ , the electrostatic potential at a distance  $x$  from the surface can be calculated by integrating the charge density from the surface up to the distance  $x$ . The surface charge density is determined from charge neutrality

which is imposed by setting the electric field to zero at  $x = D$ . The electrostatic term in the free energy  $f_{el}$  is then obtained by integrating  $pec_m h^2(x/D)\psi(x)$ .

[32] In order to interpolate between the low-salt and the salt-rich regimes, we replace  $\kappa_s^{-1}$  in the free energy, eq. 14 with  $D_{\text{eff}} \equiv 1/(1/D + \kappa_s)$ , and minimize the resulting free energy numerically.

## FIGURE CAPTIONS

**Fig. 1:** Schematic view of a polyelectrolyte solution in contact with a flat surface at  $x = 0$ . The solution contains polyelectrolyte chains and small ions. In our model, the surface is held at a constant potential.

**Fig. 2:** Adsorption profiles obtained by numerical solutions of eqs. 5,6 for several sets of physical parameters in the low-salt limit. The polymer concentration scaled by its bulk value  $\phi_b^2$  is plotted as a function of the distance from the surface. The different curves correspond to:  $p = 1$ ,  $a = 5\text{\AA}$  and  $y_s = -0.5$  in units of  $k_B T/e$  (solid curve);  $p = 0.1$ ,  $a = 5\text{\AA}$  and  $y_s = -0.5$  (dots)  $p = 1$ ,  $a = 5\text{\AA}$  and  $y_s = -1.0$  (short dashes);  $p = 1$ ,  $a = 10\text{\AA}$  and  $y_s = -0.5$  (long dashes); and  $p = 0.1, a = 5\text{\AA}$  and  $y_s = 1.0$  (dot-dash line). For all cases  $\phi_b^2 = 10^{-6}\text{\AA}^{-3}$ ,  $v = 50\text{\AA}^3$ ,  $\varepsilon = 80$ ,  $T = 300\text{K}$  and  $c_b = 0.1\text{mM}$ .

**Fig. 3:** Scaling behavior of polyelectrolyte adsorption in the low-salt regime (eqs. 11,12). (a) The rescaled electrostatic potential  $\psi(x)/|\psi_s|$  as a function of the rescaled distance  $x/D$ . (b) The rescaled polymer concentration  $c(x)/c_m$  as a function of the same rescaled distance. The profiles are taken from Fig. 2 (with the same notation). The numerical prefactors of the linear  $h(x/D)$  profile were used in the calculation of  $D$  and  $c_m$ .

**Fig. 4:** Typical adsorbed amount  $\Gamma$  as a function of (a) the charge fraction  $p$  and (b) the  $\text{pH} - \text{pK}_0$  of the solution for three different salt concentrations (eq. 17). The insets correspond to the low-salt regime (eq. 13). The parameters used for  $\varepsilon$ ,  $T$  and  $v$  are the same as in Fig. 2, while  $y_s = -0.5$  and  $a = 5\text{\AA}$ . The bulk concentration  $\phi_b^2$  is assumed to be much smaller than  $c_m$ . The numerical prefactors of the linear  $h(x/D)$  were used.

**Fig. 5:** The effect of salt concentration on the adsorption. The solid curves correspond to the scaling relations in the salt-rich regime (eqs. 15,17) and the dashed curves correspond to a simple numerical interpolation between the salt-rich and the low-salt regimes. (a) Adsorbed amount  $\Gamma$  as a function of the salt concentration  $c_b$  (eq. 17) for  $p = 0.01$  and  $0.25$ . (b) Adsorption length  $D$  as a function of the salt concentration  $c_b$  (eq. 15) for  $p = 0.1$ . The Debye-Hückel screening length  $\kappa_s^{-1}$  is also plotted (dots). The low-salt (salt-rich) regime applies when  $D \ll \kappa_s^{-1}$  ( $D \gg \kappa_s^{-1}$ ). The parameters used are:  $\varepsilon = 80$ ,  $T = 300\text{K}$   $v = 50\text{\AA}^3$ ,  $a = 5\text{\AA}$ ,  $y_s = -2.0$  and the numerical prefactors of the linear  $h(x/D)$ .

**Fig. 6:** Schematic diagram of the different adsorption regimes as function of the charge fraction  $p$  and the salt concentration  $c_b$ . Three regimes can be distinguished: (i) the low-salt regime  $D \ll \kappa_s^{-1}$ ; (ii) the salt-rich regime (SR I)  $D \gg \kappa_s^{-1}$  for weak polyelectrolytes  $p \ll p^* = (c_b v)^{1/2}$ ; and (iii) the salt-rich regime (SR II)  $D \gg \kappa_s^{-1}$  for strong polyelectrolytes  $p \gg p^*$ .



Fig. 1

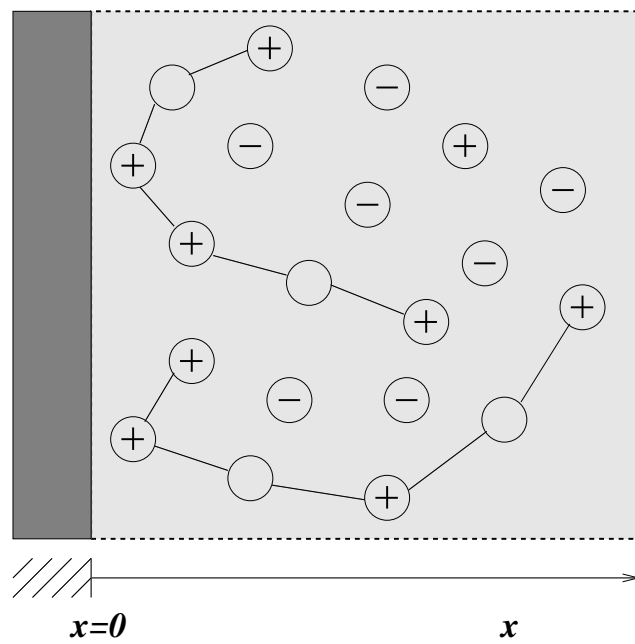


Fig. 2

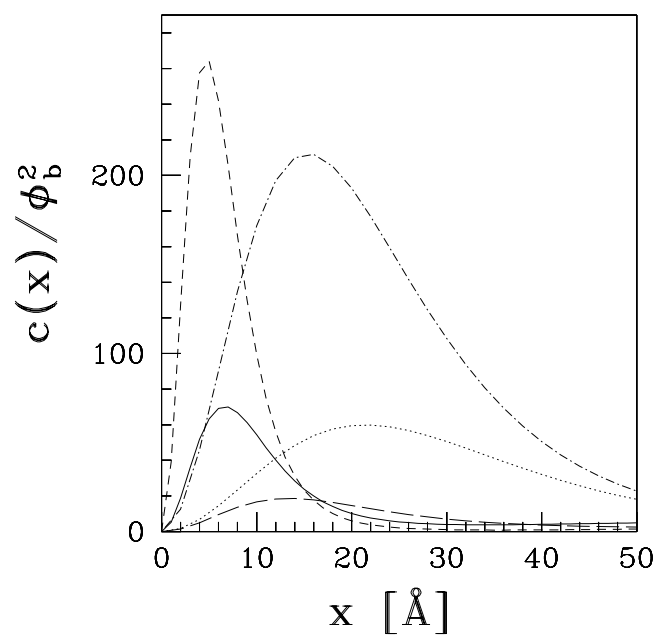


Fig. 3a

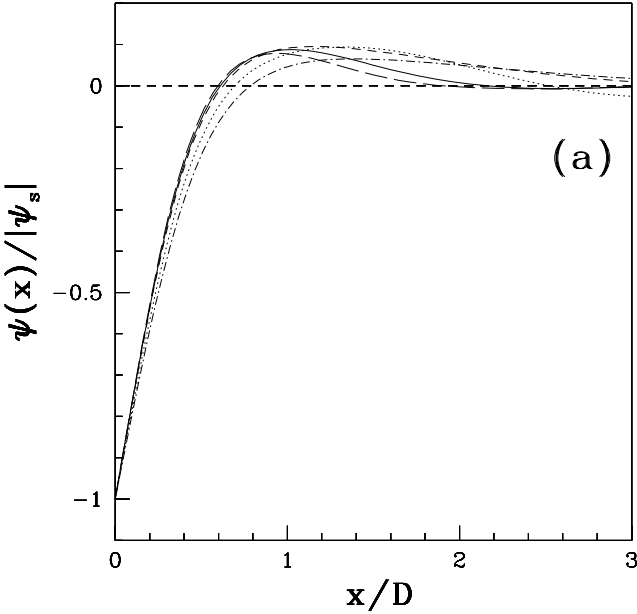


Fig. 3b

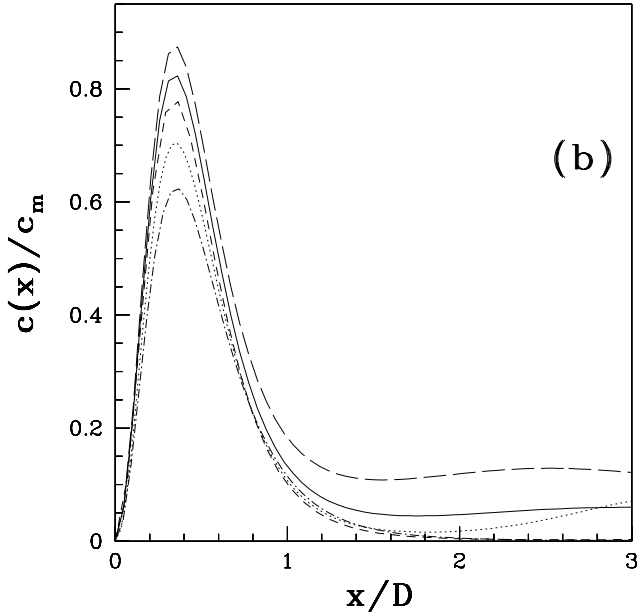


Fig. 4a

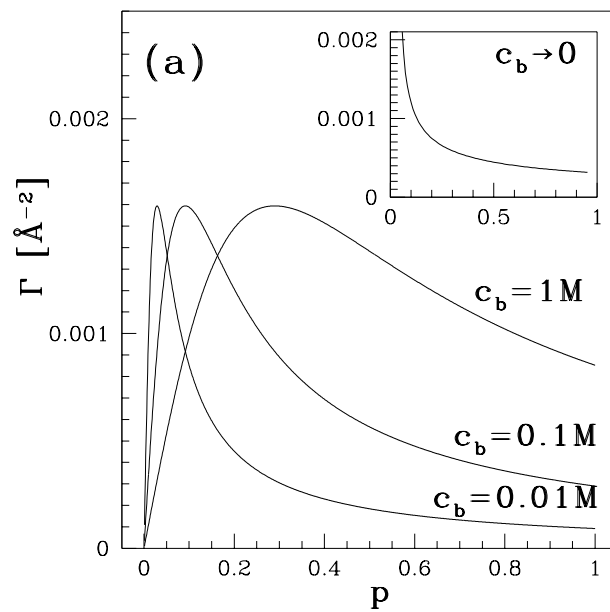


Fig. 4b

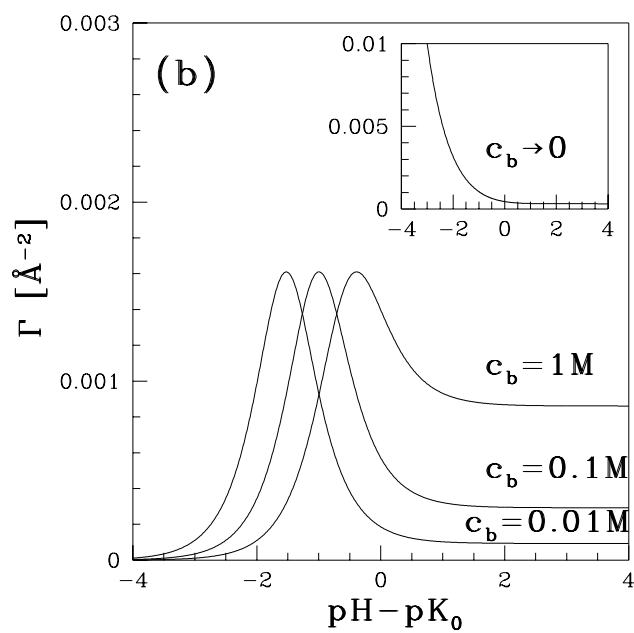


Fig. 5a

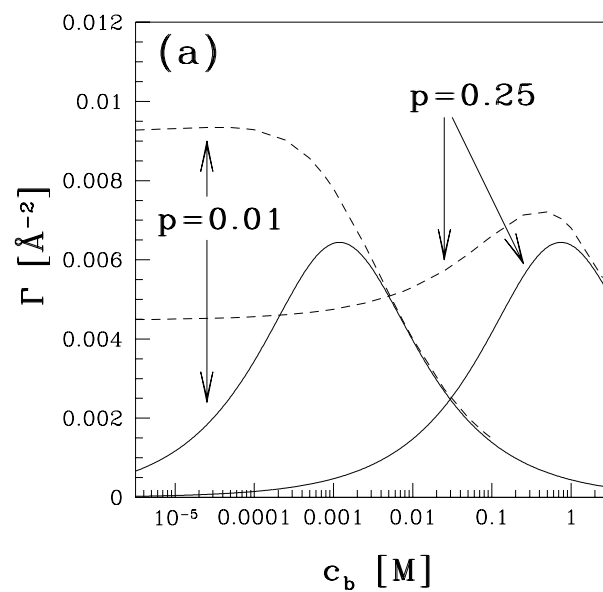


Fig. 5b

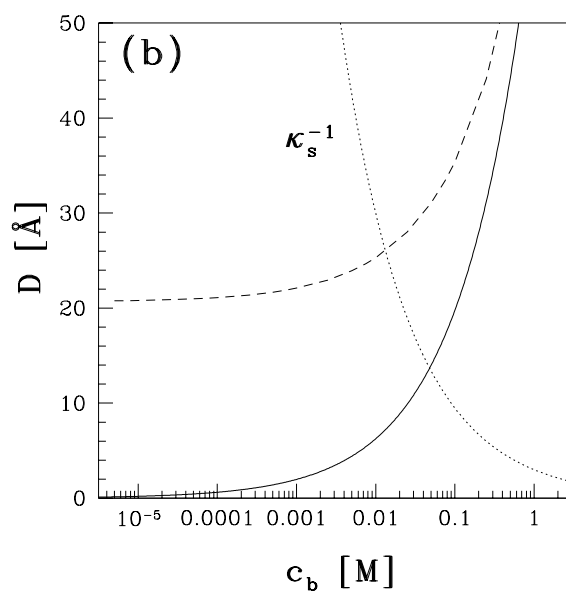


Fig. 6

